# Comparison of computational models for jointed rock mass through analysis of large-scale cavern excavation

# Comparaison de modèles numériques de masses rocheuses fissurées utilisés pour l'analyse des excavations à grande échelle

# Ein Vergleich von numerischen Modellen für gerissenen Felsen mittels Berechnungen für die Herstellung großer Felshohlräume

Hideyuki HORII, Univ. of Tokyo, Haruhiko UNO, Tokyo Electric Power Services Co., Hidenori YOSHIDA, Univ. of Tokyo, Shinichi AKUTAGAWA, Kobe Univ., Yasuo UCHIDA, NEWJEC Inc., Seiji MORIKAWA, Kajima Co., Tadashi YAMABE, Saitama Univ., Hiroyuki TADA, Shimizu Co., Takashi KYOYA, Tohoku Univ., Fumio ITO, Taisei Co.

ABSTRACT: Six analysis methods for jointed rock mass recently developed in Japan are compared. Analysis of the cavern excavation for Shiobara power station of Tokyo Electric Power Company is carried out and input parameters for each method are determined so that the measurement data are best reproduced. Numerical results are compared with measured data and the dominant mechanism that results in the characteristic behaviors of rock mass is investigated.

RÉSUMÉ: Six méthodes d'analyse de roche agglomérées récemment développées au Japon sont comparées: L'analyse de l'excavation souterraine de la centrale électrique de Shiobara (Tokyo Electric Power Company) est détaillée et les paramètres d'entrée pour chaque méthode sont déterminés de manière à reproduire au mieux les données mesurées. Les résultats numériques sont comparés aux données mesurées et le mécanisme dominant qui caractèrise le comportment de la roche est étudié.

ZUSAMMENFASSUNG: Sechs analytische Methoden für geklüftete Felsmassen (Diskontinuum), neulich entwickelt in Japan, werden verglichen. Voruntersuchungen für den Felsausbruch des Kavernen-Kraftwerks Shiobara (Tokyo Electric Power Company) werden durchgeführt. Die Eingabeparameter für die einzelnen Methoden werden so bestimmt, daß die Meßergebnisse am besten reproduziert werden können. Die numerischen Ergebnisse werden mit den Meßdaten verglichen und der dominante Mechanismus, der das typische Verhalten von Felsmassen bestimmt, wird untersucht.

## 1 INTRODUCTION

This paper reports the results of research activities in a committee in Japan Society of Civil Engineers. In Japan more than 50 caverns for underground power station have been constructed. In order to realize safe and economic design and construction, it is necessary to develop an analysis method that can accurately predict the behavior of rock mass during excavation. Once such a method is established, survey and test methods will be improved to supply input parameters and the design and construction control methods will be advanced. The first step for the rational design and construction is the improvement of the analysis method. Based on such an idea, analysis methods for jointed rock mass recently developed in Japan are compared in the present study. NAPIS (Strain-softening analysis considering the joint failure), MBC (Micromechanics Based Continuum) model, EQR (Equivalent Rock) model, Multiple Yield model, Crack Tensor model, and Damage Tensor model are employed.

Analysis of the cavern excavation for Shiobara power station of Tokyo Electric Power Company is carried out and input parameters for each method are determined so that the measurement data are best reproduced. The determined input parameters are compared to discuss the differences among the employed methods. Furthermore, the results of the analysis of the cavern excavation for Shiobara power are compared. Time histories of displacements on the cavern wall and in the rock mass are compared with measured data and it is investigated whether the characteristic behaviors are reproduced or not by each method. Considering the connection between analysis results and the mechanism adopted in the model, the dominant mechanism, which results in the characteristic behaviors of rock mass, is investigated. The fractured region, distribution of joint deformations, principal stress, tangential stiffness, and maximum shear strain, time history of stress and strain at different points are also compared and common/different features among the employed methods are discussed. A part of results is presented in this paper because of the limitation in space.

## 2 ANALYSIS METHODS FOR JOINTED ROCK MASS

Six analysis methods for jointed rock mass recently developed in Japan are employed. They account of the behaviors of dominant joints in different ways.

### 2.1 *NAPIS*

NAPIS (Strain-softening analysis considering joint failure) considers the failure of one dominant joint set and the nonlinear behavior of base rock (jointed rock mass surrounding the dominant joints) followed by stress reduction after a peak stress. Mohr-Coulomb conditions are assumed for the failure of both base rock and dominant joint. The tangent moduli of base rock and dominant joint before the peak point are given with power laws of a ratio of the Mohr circle's radius to the distance from the center of the Mohr circle to the failure curve. After the failure condition is satisfied the stress is reduced to the residual stress for the base rock. The critical stress is maintained for the failed joint.

### 2.2 *MBC (Micromechanics Based Continuum) model* [1)]

In MBC model, jointed rock mass is replaced with an equivalent continuum body whose constitutive equation is obtained from the relationship of the average stress and average strain over a representative volume element. To derive the average strain, the displacement jump along a joint is evaluated by embedding one joint of a finite length which has undulation of a zigzag shape inside a homogeneous material equivalent to the surrounding rock mass. Sliding along a part of the joint surface leads to opening along the other part. Due to the constraint by the surrounding rock mass, a finite value of the displacement jump along the joint is obtained. The process is repeated for all sets of dominant joints. The derived constitutive relationship directly reflects the orientation and spacing of the dominant joints and presents strong induced anisotropy.

### 2.3 *EQR (Equivalent Rock) analysis*

EQR analysis is based on a compliance model which assumes multiple sets of infinite flat planes (lines in 2D) with equal spacing. After Mohr-Coulomb fracture criterion is satisfied, normal and shear stiffnesses are introduced for the fractured joint. The compliance of the jointed rock mass is obtained as a sum of compliances for the base rock and each set of joints.

### 2.4 *Multiple Yield model*

Multiple yield model is also a type of the compliance model with sets of infinite flat joints of equal spacing. The base rock is modeled as an elasto-perfect-plastic material with Mohr-Coulomb yield criterion. Normal and shear stiffness (elastic spring) are assumed for joint deformations before yielding. Perfect plasticity is assumed after Mohr-Coulomb yield criterion is satisfied along a set of joints.

### 2.5 *Crack Tensor model*[2)]

In Crack Tensor model, the compliance tensor of the jointed rock mass is given as a sum of the elastic compliance tensor of the base rock and that corresponding to the crack deformation. The crack compliance (fourth order tensor) is explicitly expressed in terms of the normal and shear stiffness of joints and the joint size and components of second and fourth order crack tensors. It is derived based on the statistical consideration of the deformation of cracks that intersect an arbitrary line drawn in the jointed rock mass. The crack tensor is defined in terms of the size of the joint and components of the unit vector normal to the joint. While the dependence of the joint stiffness on the stress can be introduced, constant joint stiffness is assumed in this study and the jointed rock mass is modeled as a linear anisotropic material.

### 2.6 *Damage Tensor model*[3)]

Damage Tensor model is based on a concept that the effective cross section of the material is reduced due to the damage. Damage tensor for jointed rock mass is defined as a second order tensor expressed in terms of area and density of joint and unit normal vector. When all the possible discontinuities are separated and the rock mass is broken into fundamental element, the damage tensor is equal to the identity tensor. The effective stress acting on the effective area is expressed in terms of the damage tensor, and by applying the generalized Hook's law to the effective stress and strain, the constitutive equation for the jointed rock mass is derived.

## 3 ANALYSIS OF SHIOBARA POWER STATION CAVERN

### 3.1 *Outline of Shiobara power station cavern*

The Shiobara power station cavern constructed by Tokyo Electric Power Company is a large cavern of pumped storage power station with a maximum output of 900 MW. Surrounding rock mass is mainly rhyolite which contains platy joint and columnar joint. The cavern is at the depth of 200 m and the three principal stresses are 5.0, 3.9, and 2.8MPa. The elastic modulus of rock mass is 2.9-3.9GPa and strength parameters are c=1MPa and $\phi$=45°. The axial compressive strength and elastic modulus of the intact rock are 58.8-137.2 (ave. 83.3) MPa and 25.5-69.6 (ave. 42.1) GPa, respectively.

The cavern has a width of 28 m, a height of 51 m, a length of 161 m and the amount of the excavation of rock mass is more than 190,000 $m^3$. Figure 1 shows the cross section of the cavern and the location of displacement transducers.

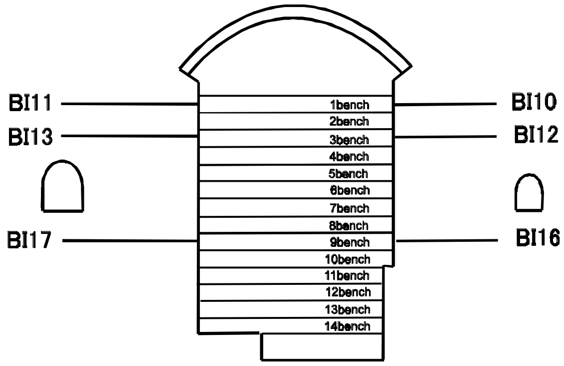


Fig. 1 Cross-section of cavern and location of displacement transducers

### 3.2 *Conditions for the numerical analysis*

Initial stress, strike and dip angles and average spacing of dominant joints for two-dimensional analysis are determined based on reported data. The initial maximum principal stress is 4.7MPa in the direction of 15 degrees counterclockwise from vertical direction. The minimum principal stress is 3.5MPa. A joint set having its strike perpendicular to the cavern axis (N40E) is considered to be less important for the deformation of side cavern walls, and joint sets having their strike (N25E60S, N30E30N and N40E60N) parallel to the axis are considered. Symbol 60R in Tab. 1 indicates a dip angle of 60 degrees down to right.

Table 1 Dip angle and average spacing of dominant joints

| Joint set | Dip angle | Ave. spacing |
|---|---|---|
| I | 60R | 30cm |
| II | 60L | 100cm |
| III | 30L | 100cm |

### 3.3 *Determined Input parameters*

Analyses of the cavern excavation for Shiobara power station are carried out with the six analysis methods and input parameters for each method are determined so that the measurement data are best reproduced. Table 1 summarizes the determined input parameters.

It is seen that all the methods treat the behaviors of dominant joints, but the extent to be covered as the behaviors of dominant joints is different. Methods that use large values of elastic modulus for the base rock close to that of intact rock are considered to attribute inelastic behaviors to the dominant joints, while in the other methods some portion of behaviors of discontinuities is modeled by the behaviors of the base rock.

Four models include fracture conditions of the joints. It means that the expansion of the region, inside which the joints are fractured, the stiffness is reduced, and induced anisotropy may dominate, would be predicted by those methods. MBC model considers dominant joints with undulation embedded in jointed rock mass, and the size of the dominant joints plays an important role. The shear deformation of joints results in the dilatation due to the undulation. In the other methods the joint behaviors are characterized by the joint stiffness. The effect of the joint size in the MBC model can be represented with a joint stiffness that is a function of the joint size.

## 4 COMPARISON OF NUMERICAL RESULTS

In Figs. 2, the time history of relative displacement near the cavern wall are shown and measured data (solid line) and numerical results are compared. Figs. 3 show the distribution of displacement along each measurement line at the completion of the whole excavation. The characteristic behaviors of rock mass

Table 2 Determined input parameters

| | Method | ①NAPIS | ②MBC | ③EQR | ④MYM | ⑤CTM | ⑥DTM |
|---|---|---|---|---|---|---|---|
| Base Rock | E(GPa) | $E_i$=9.8 Non-linear | 5.0 | 42.1 | 2.9 | 39.2 | 19.6 |
| | $E_f$(GPa) | 4.9 | — | — | 1.5 | — | — |
| | ν | 0.25 | 0.25 | 0.14 | 0.25 | 0.25 | 0.25 |
| | Peak Strength (MPa) | $C_p$=2.2 $\phi_p$=55.3° | — | — | C=1.2 $\phi$=45° | — | — |
| | Residual Strength (MPa) | $C_r$=0.7 $\phi_r$=52.1° | — | — | — | — | — |
| | Tensile Strength (MPa) | 1.5 | — | — | 0.1 | — | — |
| Joint Properties | Joint Orientation Joint Spacing | -60° 0.3m | -60° 0.3m<br>60° 1.0m<br>30° 1.0m | -60° 0.3m<br>60° 1.0m<br>30° 1.0m | -60° 0.3m<br>60° 1.0m<br>30° 1.0m | 45° | -60° 0.3m<br>60° 1.0m<br>30° 1.0m |
| | Other Joint Parameters | — | L=2.0,0.5,0.5 m α=5° | — | — | $F_0$=10 (Joint Density) | $C_n$=1,$C_s$=1 |
| | $k_n$ (MPa/cm) | ∞ | — | 98 | $29.4\times10^3$ | $19.6\times10^3$ | — |
| | $k_s$ (MPa/cm) | $k_{s0}=10\times\sigma_n$ Non-linear | — | $15\times\sigma_n$ | $11.8\times10^3$ | $2.5\times10^3$ | — |
| | Fracture Strength | $C_j$=0 $\Phi_j$=45° | $C_j$=0 $\Phi_j$=35, 50, 50° | $C_j$=1.0 $\Phi_j$=35° | $C_j$=0 $\Phi_j$=35° | — | — |
| | Support System | PS Anchor | PS Anchor | | | | |

seen from the measured data in Figs. 2 and 3 are summarized as follows.

① Displacement increases continuously during the bench excavation at lower levels.

② The displacement is anti-symmetric and larger at the left side wall.

③ Displacement increases drastically near the cavern wall at the upper part of the left side, while the increase starts from 10-15m depth. Linear distribution of displacement is observed at the right side.

④ The displacement is almost constant near the cavern wall.

It is investigated whether those characteristic behaviors are captured by each numerical method or not.

The tendency ② is captured more or less by most of the employed methods. This anti-symmetry is considered to be the result of the inclined principal stress and the behavior of the joint set Ⅰ(60R) which has a smaller spacing and is likely to slide on the left side of the cavern. NAPIS considers only this set of joints. MBC assumes a larger size and smaller fracture angle for the joint set Ⅰ. Those means emphasize the anti-symmetry of the deformation.

The characteristic behavior ① is clearly seen in Figs. 2. MBC captures this behavior while results by other methods show that the displacement stops to increase at earlier stage and even decreases during the excavation of lower benches. The reason why MBC reproduces the continuous increase in displacement at the upper part of the left side is the following.

In MBC, parameters for the joint set Ⅰ are selected in addition to its smaller average spacing so that the joints of set Ⅰ start to slide earlier and the amount of sliding is larger. From geometrical condition the sliding of the joints of set Ⅰ dipping down to right is easier at the left side of the cavern. The maximum principal stress, which is slightly inclined to the joints of set Ⅰ, also promote their sliding.

The displacement along BI13 starts to increase when the third bench at the same level is excavated. Initially the joints of set Ⅰ are active while other sets of joints are inactive at this stage. When the seventh bench is excavated, the joints of set Ⅱand Ⅲ dipping down to left become active around the area between the abutment and the side tunnel at the left side of the cavern. The area inside which all sets of joints are active continue to expand during the following excavation steps. The rock mass whose multiple sets of joints are active has a very small stiffness leading to large deformation. This is the mechanism of the continuous increase in the displacement at the left side of the cavern.

The tendency ③ seen in BI11 of Figs. 3 is also reproduced by the MBC model. Near the wall surface up to a depth of 5m, large displacement is observed. In the MBC analysis, all sets of joints are active in this area. In the area deeper than 5m only set Ⅰ or no sets are active. This explains the characteristic behavior ③ seen along BI11.

## 5 CONCLUDING REMARKS

Only limited results are presented in this paper. The shape and size of the joint fracture zone, distribution of stresses, maximum shear strain, tangent stiffness of rock mass, histories of stress and strain at different points, and other quantities by different methods are compared to identify the relationship between the characteristic phenomena during cavern excavation and the mechanism treated in each numerical method.

Results of excavation analyses of caverns with different shapes are also compared to clarify the effect of cavern shape. The main issue under discussion is the application of these achievements to engineering practice, which includes the design method based on the advanced numerical method for jointed rock mass.

Acknowledgement

This paper reports the results of research activities in the sub-committee on technology for large scale cavern excavation, the committee of civil engineering for energyequipment (chaired by H. Takagi), Japan Society of Civil Engineers. Authors are thankful to Tokyo Electric Power Co., Ltd. for the kind data provision.

References

1) H. Yoshida and H. Horii "Micromechanics-based continuum analysis for the excavation of large-scale underground cavern" Proc. of SPE/ISRM Rock Mech. in Petro. Eng., 1 (1998) 209-218.
2) M. Oda, T. Yamabe, Y. Ishizuka, H. Kumasaka and H. Tada " Elastic stress and strain in jointed rock masses by means of crack tensor analysis" Rock Mech. and Rock Eng., 26 (1993) 89-112.
3) T. Kawamoto, Y. Ichikawa, and T. Kyoya "Deformation and fracturing behaviouof discontinuous rock mass and damage mechanics theory" Int. J. Num. Anal. Meth. Geomech., 12 (1988) 1-30.

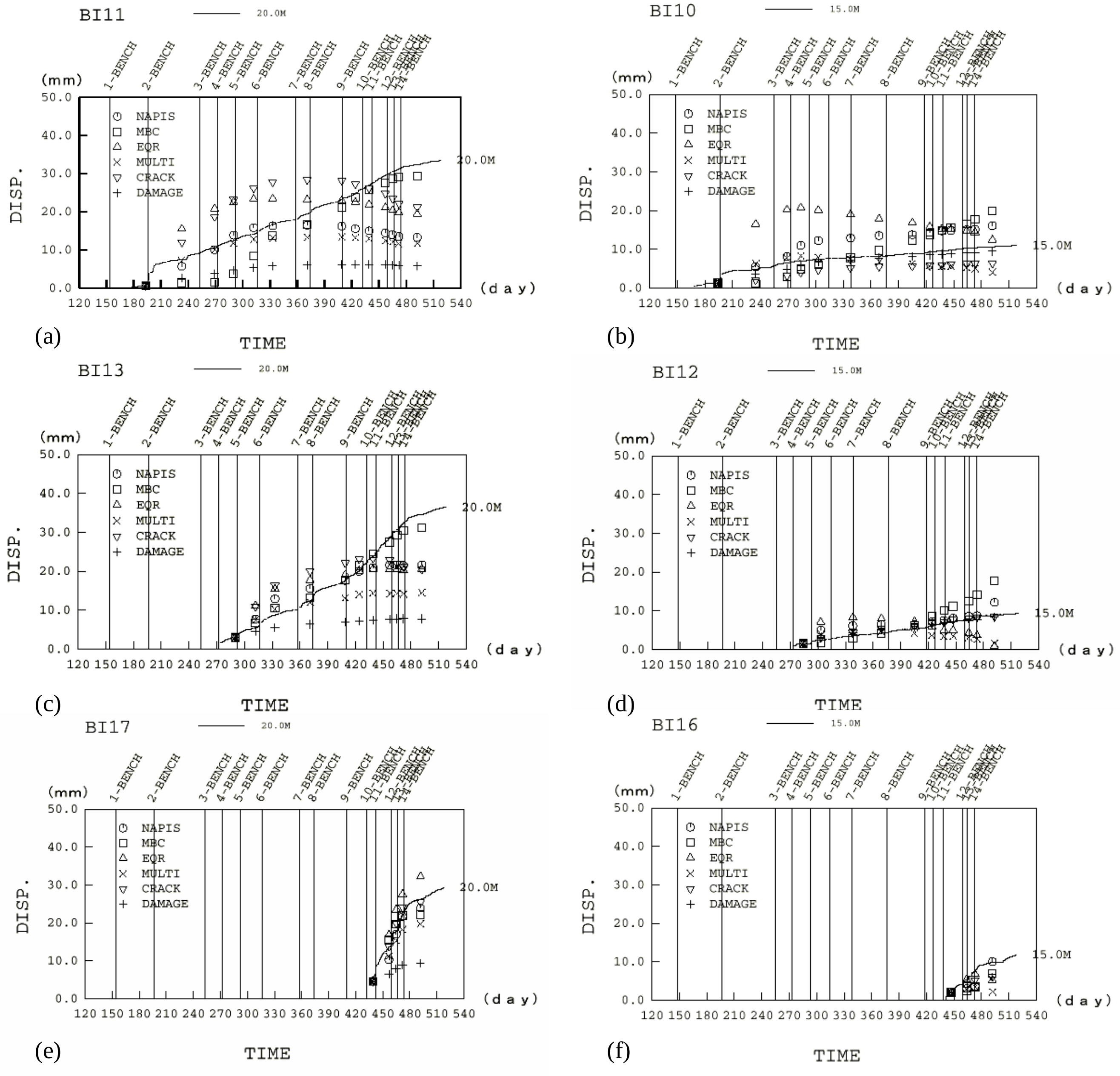


Figs. 2 Time history of of relative displacement near the cavern wall.

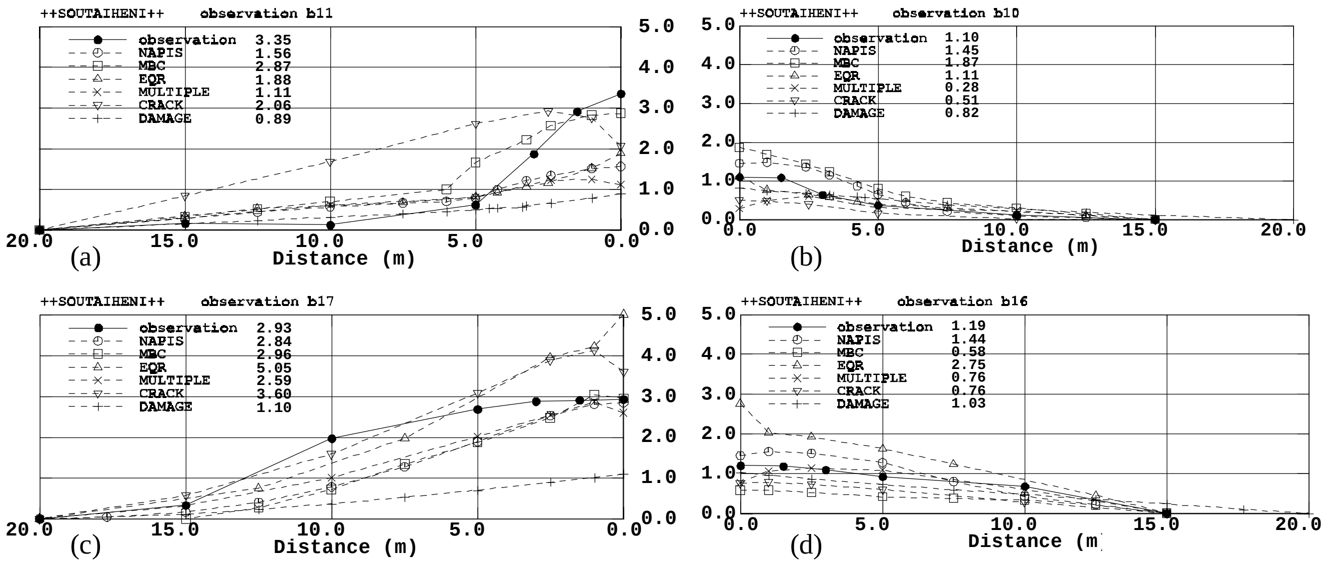


Figs. 3 Distribution of displacement along each measurement line at the completion of the whole excavation: (a) BI11, (b) BI10, (c) BI17, (d) BI16.